STATE OF THE CLIMATE IN 2017

Special Supplement to the
Bulletin of the American Meteorological Society
Vol. 99, No. 8, August 2018

STATE OF THE CLIMATE IN 2017

Editors

Jessica Blunden
Derek S. Arndt
Gail Hartfield

Chapter Editors

Peter Bissolli
Howard J. Diamond
Robert J. H. Dunn
Catherine Ganter
Nadine Gobron
Martin O. Jeffries
Gregory C. Johnson
Tim Li
Ademe Mekonnen
Emily Osborne
Jacqueline A. Richter-Menge
Ahira Sánchez-Lugo
Ted A. Scambos
Carl J. Schreck III
Sharon Stammerjohn
Diane M. Stanitski
Kate M. Willett

Technical Editor

Mara Sprain

AMERICAN METEOROLOGICAL SOCIETY

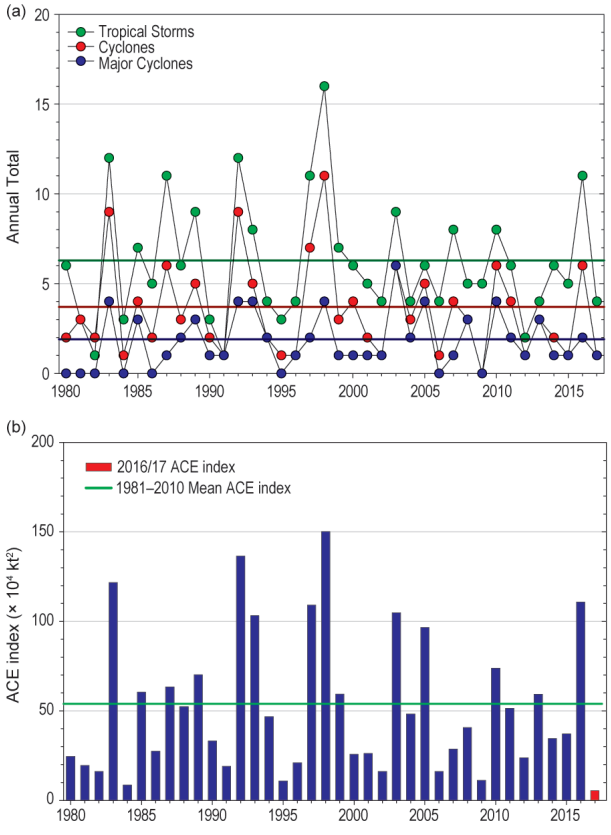

Fig. 4.35. Annual TC statistics for the southwest Pacific for 1980–2017: (a) number of tropical storms, cyclones, and major cyclones and (b) estimated annual ACE index (in $kt^2 \times 10^4$; Bell et al. 2000). The 1981–2010 means (horizontal lines) are included in both (a) and (b). Note that ACE is estimated due to lack of consistent 6-h sustained winds for each storm.

(ii) Landfalling and other significant TCs

Tropical Cyclone Alfred developed as a tropical low on 16 February in the southern Gulf of Carpentaria. The low gradually intensified into a category 1 TC on 20 February and remained at TC strength before weakening approximately 24 hours later. Alfred was the first tropical cyclone to make landfall in Australia's Northern Territory since 2015. Alfred's peak 10-minute wind speed was 46 kt (24 m s^{-1}) and its lowest central pressure was 994 hPa.

Tropical Cyclone Bart was a short-lived cyclone which lasted from 19 to 22 February, forming south of Samoa and traveling southeast to the south of the southern Cook Islands. Bart reached category 1 status, where peak 10-minute sustained wind speeds were 40 kt (21 m s^{-1}) and minimum central pressures reached 994 hPa.

Tropical Cyclone Cook was named on 8 April after forming northeast of Vanuatu. Some trees were felled and power was cut to some residents in Port Vila, Vanuatu. Cook brought heavy rain and destructive winds to parts of New Caledonia, where one fatality was reported. Cook also caused wind damage to trees and infrastructure in parts of New Zealand's North Island, one week after ex-Tropical Cyclone Debbie caused major flooding in the same area. Cook achieved category 3 status with 10-minute sustained winds of 84 kt (43 m s^{-1}) and a minimum central pressure of 961 hPa.

Tropical Cyclone Donna formed to the north of Vanuatu on 1 May, which is just past the traditional end of the season (30 April). It achieved named storm status on 3 May, and late on 4 May it began to show a clear eye and was upgraded to a category 3 tropical cyclone. On 6 May, Donna was upgraded to category 4 status. It weakened to a category 3 storm later on 6 May but then strengthened again to category 4 status the next day before being upgraded to category 5 status on 8 May. Donna's peak 10-minute sustained wind speed reached 111 kt (57 m s^{-1}) and its lowest minimum central pressure was 935 hPa. As a result, Donna became the strongest out-of-season TC on record for May in the southwest Pacific. Donna degraded quickly to tropical low strength on 10 May. The storm caused significant damage in Vanuatu. Entire villages across the Torres Islands in Torba Province were forced to seek shelter from the storm in caves. Throughout the province, many buildings were destroyed or severely damaged. On the island of Efate, heavy rainfall led to flooding of low-lying areas. Structures collapsed in Port Vila because they were undermined during flash floods. Across the northern half of Vanuatu, crops sustained significant damage and communications were severed with the rest of the country. In the Temotu Province of the Solomon Islands, Donna caused two fatalities. In New Zealand, Donna's remnants produced heavy rain over much of the North Island and the west coast of the South Island on 11–12 May.

The season concluded with Tropical Cyclone Ella, which formed southwest of American Samoa on 9 May. Just three hours later, the system intensified into a category 1 TC, and it reached category 2 status on 10 May. Its peak 10-minute sustained wind speed was 59 kt (31 m s^{-1}) with a minimum central pressure of 977 hPa.

g. Tropical cyclone heat potential—G. J. Goni, J. A. Knaff, I.-I. Lin, and R. Domingues

This section summarizes the changes in upper ocean thermal conditions within the seven tropical cyclone (TC) basins (see Table 4.1), using tropical cyclone heat potential (TCHP; Goni and Trinanes 2003)

as the main parameter. The assessment presented here focuses on the vertically-integrated upper ocean temperature conditions during the TC season of each ocean basin with respect to the long-term mean and to values observed during the previous year. TCHP is defined as the excess heat content contained in the water column between the sea surface and the depth of the 26°C isotherm. This parameter has been linked to TC intensity changes (Shay et al. 2000; Mainelli et al 2008; Lin et al. 2014) with TCHP values above 50 kJ cm^{-2} providing the necessary ocean conditions for Atlantic hurricane intensification when favorable atmospheric conditions are present. The magnitude of the TCHP has been identified as modulating the effective SST under a TC during air–sea coupling due to latent and sensible heat fluxes (Mainelli et al. 2008; Lin et al. 2013). In addition, improved temporal and spatial sampling of the ocean has been shown to lead to the correct representation of the upper ocean density field (Domingues et al. 2015), which in turn led to reducing the error in hurricane intensification forecasts within operational numerical models (Dong et al. 2017). Fields of TCHP show high spatial and temporal variability associated mainly with oceanic mesoscale features, year-to-year variability (e.g., ENSO), or long-term decadal variability. The assessment of this variability on various timescales can be accomplished using a combination of satellite altimetry and in situ observations (Goni et al. 1996; Lin et al. 2008; Goni and Knaff 2009; Pun et al. 2013).

To assess year-to-year variations in TCHP, two fields are presented. First, Fig. 4.36 presents TCHP anomalies (departures from the 1993–2016 mean values) for the primary months of TC activity in each hemisphere: June–November in the Northern Hemisphere, and November 2016–April 2017 in the Southern Hemisphere. TCHP anomalies generally show large variability within and among the TC basins. Figure 4.37 shows the differences of TCHP between this season (2017) and last year (2016).

Most basins exhibited positive TCHP anomalies in 2017 (Fig. 4.36), except for a small region just east of 60°E in the southwest Indian basin. Above-average TCHP in most basins provided anomalously favorable ocean conditions for the intensification of TCs. In the tropical Atlantic basin, TCHP values observed in 2017 were approximately 10% larger than the long-term mean, consistent with the above-normal activity there. Meanwhile, the western North Pacific (WNP) basin had below-normal activity despite TCHP values being over 30% larger than the mean conditions. This is explained because the number of TCs in the WNP during a season is more closely related to atmospheric dynamics (Lin and Chan 2015) than to upper ocean conditions.

In the Gulf of Mexico, TCHP anomalies ranged between –10 and 20 kJ cm^{-2} with the spatial distribution largely determined by the mesoscale field, such as the extension of the Loop Current, and cold cyclonic features. In the eastern Gulf of Mexico, prominent intrusion of the Loop Current caused TCHP values in 2017 to be 50% larger than the mean; a noticeable change with respect to conditions in 2016, which was characterized by a small intrusion of the Loop Current. The TCHP in the western Gulf of Mexico once again exhibited positive anomalies, with values approximately 30% larger than the long-term mean. Compared to 2016, TC activity increased in the Gulf of Mexico in 2017 with a total of five TCs including the rapidly intensifying category 4 Hurricane Harvey.

In the eastern North Pacific (ENP) basin, TCHP values were 10–20 kJ cm^{-2} above the long-term mean associated with a continued positive phase of the Pacific decadal oscillation (Zhang et al. 1997). Anomalies observed in 2017, however, were not so large as the values observed in 2016. This change is largely due to the ENSO conditions described in Section 4b. As a consequence, average TC activity was observed in the ENP, with nine hurricanes in 2017 (Fig. 4.36).

The TCHP in the WNP basin is also closely modulated by ENSO variability (Lin et al. 2014; Zheng et

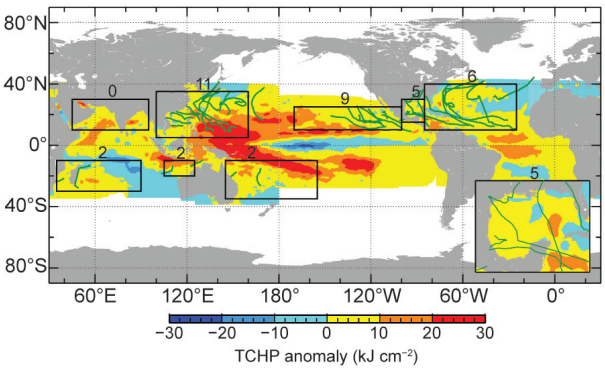

Fig. 4.36. Global anomalies of TCHP (kJ cm^{-2}) corresponding to 2017 computed as described in the text. Boxes indicate the seven regions where TCs occur: from left to right, southwest Indian, north Indian, west North Pacific, southeast Indian, South Pacific, East Pacific, and North Atlantic (shown as Gulf of Mexico and tropical Atlantic separately). Green lines indicate the trajectories of all tropical cyclones reaching at least Saffir–Simpson category 1 during Nov 2016–Apr 2017 in the SH and Jun–Nov 2017 in the NH. The numbers above each box correspond to the number of category 1 and above cyclones that traveled within each box. Gulf of Mexico conditions during Jun–Nov 2017 are shown in the inset in the lower right corner.

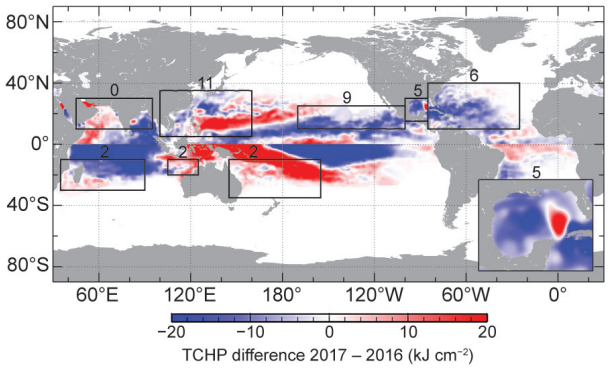

Fig. 4.37. TCHP differences (kJ cm^{-2}) between 2017 and 2016.

al. 2015). For example, from the 1990s to 2013 the WNP experienced a long-term decadal surface and subsurface warming associated with more prevalent La Niña-like conditions (Pun et al. 2013; England et al. 2014; Lin and Chan 2015). With the ENSO conditions during 2014/15, however, this warming trend stopped, but it recovered again in 2016. In 2017, further warming of the WNP basin and TCHP anomalies as large as 40 kJ cm^{-2} were observed, which is approximately 30% larger than the long-term mean for the region. However, the overall TC activity over the WNP basin was not so active as in 2016 due to less favorable atmospheric dynamic conditions (Lin and Chan 2015; Section 4f4).

For each basin, the differences in the TCHP values between this season and 2016 (Fig. 4.37) indicate that three of the seven active TC basins exhibited a decrease in TCHP values, namely the: (1) South Indian Ocean, (2) eastern North Pacific Ocean, and (3) North Atlantic Ocean basins. It is likely that lower TCHP values in the south Indian Ocean played a role in suppressing TC activity in 2016/17, which observed only one major TC during the season. However, despite showing a moderate decrease in TCHP with respect to 2016, above-normal TC activity in terms of category 4 and 5 storms was observed in the tropical Atlantic and Gulf of Mexico, with the development of six major Atlantic hurricanes. Intense hurricane activity in the Atlantic during the last season likely benefited from above-normal TCHP in the tropical Atlantic and Gulf of Mexico (Fig. 4.36) combined with favorable atmospheric conditions associated with a cool neutral ENSO state, which is known for decreasing vertical wind shear and trade wind intensity, supporting TC development and intensification (Gray 1984). In addition, atmospheric conditions in the tropical Atlantic, as described in Section 4f2, favored the development of intense TC activity (Bell et al. 2017b). Hurricanes Irma and Maria, for example, had sustained winds that reached 160 kt (67 m s^{-1}) and 150 kt (72 m s^{-1}), respectively. Both storms were well observed by reconnaissance aircraft equipped with stepped frequency microwave radiometers that provide accurate estimates of surface wind speeds (Uhlhorn and Black 2003).

An increase in TCHP values with respect to the previous season was recorded in the North Indian Ocean (Arabian Sea), southeast Indian Ocean, southwest Pacific, and WNP ocean basins. The largest changes with respect to the previous season were observed in the south Indian Ocean basin, and in the WNP north of 10°N, with differences above –20 and 20 kJ cm^{-2} respectively. Super Typhoon Noru was the fifth named storm to develop during the season and experienced rapid intensification from tropical storm into a category 5 TC as it moved from an area of low TCHP (~40 kJ cm^{-2}) into an area with TCHP values of ~80 kJ cm^{-2}.

Ocean conditions of four of the six major hurricanes (Harvey, Irma, Jose, and Maria) of the Atlantic basin are described here. Data from the ocean observing system, including observations from underwater gliders that were deployed to collect data in support of operational hurricane intensity forecasts, are presented here (Fig. 4.38). These observations were collected because a better representation of the upper ocean temperature and salinity conditions has been shown to reduce the error in Atlantic hurricane intensity forecasts within the NOAA experimental HYCOM-HWRF operational model (Dong et al. 2017). Ocean conditions before, during, and after the passage of these hurricanes were continuously monitored by some of these gliders.

Hurricane Harvey traveled through the Caribbean Sea south of Puerto Rico on 20 August, where the upper ocean exhibited TCHP values higher than 80 kJ cm^{-2}. In this area, underwater glider data showed that a relatively shallow mixed layer favored cooling of the upper ocean, which together with the moderate wind shear contributed to its lack of intensification in that region. Once it reached the Gulf of Mexico, Hurricane Harvey intensified from a tropical depression into a category 4 hurricane with 115 kt (51 m s^{-1}) winds in a period of less than 48 hours as it traveled over positive TCHP anomalies in the western Gulf of Mexico. Harvey produced the largest amount of rain on record in the continental United States, which caused extensive flooding in the Houston, Texas, metropolitan area (see Sidebar 4.3 for detailed information about the precipitation associated with Harvey).

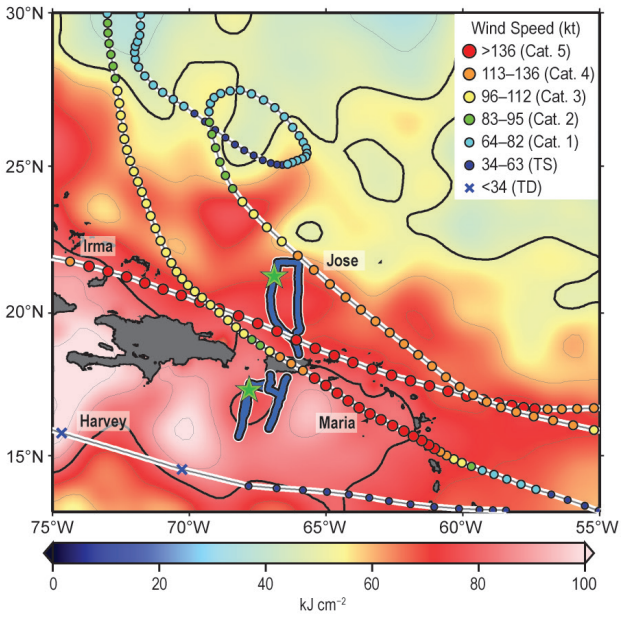

Fig. 4.38. Tracks of major Atlantic hurricanes that traveled over the Caribbean Sea and tropical North Atlantic Ocean during the 2017 hurricane season. Blue lines indicate the location of some of the underwater gliders, which were parked in fixed locations (green stars) during the passage of the major hurricanes. Background colors show values of TCHP averaged for Aug 2017, with thin contours every 10 kJ cm^{-2}, and thick contours indicate 50 kJ cm^{-2} and 80 kJ cm^{-2}, respectively.

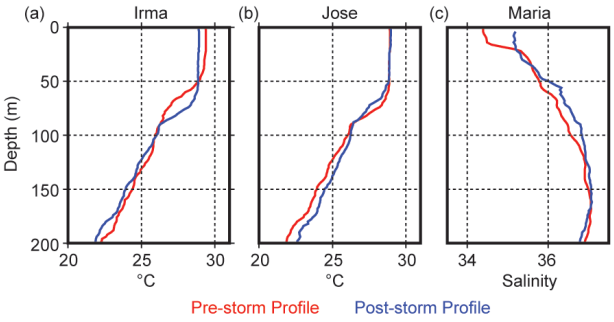

Fig. 4.39. (a), (b) Temperature (°C) and (c) salinity profiles sampled by underwater gliders before and after the passage of three major North Atlantic hurricanes (Irma, Jose, and Maria) in 2017.

Hurricane Irma, the strongest TC globally in 2017, reached its maximum intensity of 160 kt (82 m s^{-1}) on 6 September while traveling over waters north of Puerto Rico and Hispaniola that had TCHP values higher than 70 kJ cm^{-2}. Underwater glider data showed that the upper ocean conditions exhibited low salinity values at the surface, partially suppressing upper ocean mixing with colder underlying waters, similar to what happened with Hurricane Gonzalo in 2014 (Domingues et al. 2015; Dong et al. 2017), but opposite to the conditions experienced during Hurricane Harvey. Glider observations also revealed that the upper 50 m of the ocean cooled by approximately 1°C (Fig. 4.39a) as a result of storm-induced mixing.

Hurricane Jose was the third strongest Atlantic hurricane in 2017 and was the seventh longest-lived Atlantic named storm in the satellite era (since 1966). While Jose was off Puerto Rico, 2°–3° latitude to the north of where Irma traveled, its trajectory coincided at a time with the cold wake left behind by the passage of Hurricane Irma. Therefore, Jose experienced a relatively cooler and well mixed upper ocean as observed by underwater glider data (Fig. 4.39b). These cooler ocean conditions may have partly contributed to its weakening from a category 4 hurricane to category 3 during this time.

Hurricane Maria traveled through the eastern Caribbean Sea and later through the same approximate area as Irma transited the tropical North Atlantic, On 20 September, after entering the Caribbean Sea following a landfall in Dominica, Maria peaked in intensity with maximum sustained winds of 150 kt (77 m s^{-1}) and a minimum pressure of 908 hPa, making Maria the tenth-most intense Atlantic hurricane on record. When Maria's path was close to the gliders in the Caribbean Sea, these ocean observations revealed the existence of a very stable barrier layer of approximately 30-m depth (Fig. 4.39c) providing ocean conditions conducive for intensification. Maria made landfall in Puerto Rico on 20 September as an intense category 4 hurricane. Interaction with land further weakened the hurricane, though it regained some strength as it traveled over waters with TCHP values of ~70 kJ cm^{-2} north of Hispaniola (Fig. 4.38). As it traveled farther to the north it encountered lower TCHP which helped to contribute to Maria's weakening to a tropical storm on 28 September.

In summary, 2017 was characterized by higher-than-normal values of TCHP by 10%–30% over most TC basins. Overall, TCHP anomalies observed in 2017 were not so large as anomalies observed in 2016, which likely contributed to both fewer overall TCs as well as fewer category 5 TCs globally. Ocean observations during 2017 indicated that upper ocean conditions may have favored the intensification of major TCs, but atmospheric conditions (especially in the western North Pacific) were likely not as conducive for strong TCs.

h. Indian Ocean dipole—J.-J. Luo

The Indian Ocean dipole (IOD), referring to the anomalous SST gradient between the western and eastern equatorial Indian Ocean, is a major internal